The Astrophysical Journal, 706:L56–L61, 2009 November 20 doi:10.1088/0004-637X/706/1/L56

FERMI/LAT OBSERVATIONS OF LS 5039

A. A. Abdo[1,2], M. Ackermann[3], M. Ajello[3], W. B. Atwood[4], M. Axelsson[5,6], L. Baldini[7], J. Ballet[8], G. Barbiellini[9,10], D. Bastieri[11,12], B. M. Baughman[13], K. Bechtol[3], R. Bellazzini[7], B. Berenji[3], R. D. Blandford[3], E. D. Bloom[3], E. Bonamente[14,15], A. W. Borgland[3], J. Bregeon[7], A. Brez[7], M. Brigida[16,17], P. Bruel[18], T. H. Burnett[19], S. Buson[12], G. A. Caliandro[16,17], R. A. Cameron[3], P. A. Caraveo[20], J. M. Casandjian[8], E. Cavazzuti[21], C. Cecchi[14,15], Ö. Çelik[22,23,24], S. Chaty[8], A. Chekhtman[1,25], C. C. Cheung[22], J. Chiang[3], S. Ciprini[14,15], R. Claus[3], J. Cohen-Tanugi[26], L. R. Cominsky[27], J. Conrad[6,28,56], S. Corbel[8], R. Corbet[22,24], S. Cutini[21], C. D. Dermer[1], A. de Angelis[29], F. de Palma[16,17], S. W. Digel[3], E. do Couto e Silva[3], P. S. Drell[3], R. Dubois[3], G. Dubus[30,57], D. Dumora[31,32], C. Farnier[26], C. Favuzzi[16,17], S. J. Fegan[18], W. B. Focke[3], P. Fortin[18], M. Frailis[29], Y. Fukazawa[33], S. Funk[3], P. Fusco[16,17], F. Gargano[17], D. Gasparrini[21], N. Gehrels[22,34], S. Germani[14,15], B. Giebels[18], N. Giglietto[16,17], F. Giordano[16,17], T. Glanzman[3], G. Godfrey[3], I. A. Grenier[8], M.-H. Grondin[31,32], J. E. Grove[1], L. Guillemot[31,32], S. Guiriec[35], Y. Hanabata[33], A. K. Harding[22], M. Hayashida[3], E. Hays[22], A. B. Hill[30,57], D. Horan[18], R. E. Hughes[13], M. S. Jackson[28], G. Jóhannesson[3], A. S. Johnson[3], T. J. Johnson[22,34], W. N. Johnson[1], T. Kamae[3], H. Katagiri[33], J. Kataoka[36,37], N. Kawai[36,38], M. Kerr[19], J. Knödlseder[39], M. L. Kocian[3], F. Kuehn[13], M. Kuss[7], J. Lande[3], S. Larsson[28,6], L. Latronico[7], M. Lemoine-Goumard[31,32], F. Longo[9,10], F. Loparco[16,17], B. Lott[31,32], M. N. Lovellette[1], P. Lubrano[14,15], G. M. Madejski[3], A. Makeev[1,25], M. Marelli[20], M. N. Mazziotta[17], J. E. McEnery[22], C. Meurer[28,6], P. F. Michelson[3], W. Mitthumsiri[3], T. Mizuno[33], A. A. Moiseev[23,34], C. Monte[16,17], M. E. Monzani[3], A. Morselli[40], I. V. Moskalenko[3], S. Murgia[3], P. L. Nolan[3], J. P. Norris[41], E. Nuss[26], T. Ohsugi[33], N. Omodei[7], E. Orlando[42], J. F. Ormes[41], M. Ozaki[43], D. Paneque[3], J. H. Panetta[3], D. Parent[31,32], V. Pelassa[26], M. Pepe[14,15], M. Pesce-Rollins[7], F. Piron[26], T. A. Porter[4], S. Rainò[16,17], R. Rando[11,12], P. S. Ray[1], M. Razzano[7], N. Rea[44,45], A. Reimer[46,3], O. Reimer[46,3], T. Reposeur[31,32], S. Ritz[4], L. S. Rochester[3], A. Y. Rodriguez[44], R. W. Romani[3], M. Roth[19], F. Ryde[47,6], H. F.-W. Sadrozinski[4], D. Sanchez[18], A. Sander[13], P. M. Saz Parkinson[4], J. D. Scargle[48], C. Sgrò[7], A. Sierpowska-Bartosik[44], E. J. Siskind[49], D. A. Smith[31,32], P. D. Smith[13], G. Spandre[7], P. Spinelli[16,17], M. S. Strickman[1], D. J. Suson[50], H. Tajima[3], H. Takahashi[33], T. Takahashi[43], T. Tanaka[3], Y. Tanaka[43], J. B. Thayer[3], D. J. Thompson[22], L. Tibaldo[11,8,12], D. F. Torres[44,51], G. Tosti[14,15], A. Tramacere[3,52], Y. Uchiyama[3,43], T. L. Usher[3], V. Vasileiou[22,23,24], C. Venter[22,53], N. Vilchez[39], V. Vitale[40,54], A. P. Waite[3], E. Wallace[19], P. Wang[3], B. L. Winer[13], K. S. Wood[1], T. Ylinen[6,47,55], and M. Ziegler[4]

[1] Space Science Division, Naval Research Laboratory, Washington, DC 20375, USA
[2] National Research Council Research Associate, National Academy of Sciences, Washington, DC 20001, USA
[3] W. W. Hansen Experimental Physics Laboratory, Kavli Institute for Particle Astrophysics and Cosmology, Department of Physics and SLAC National Accelerator Laboratory, Stanford University, Stanford, CA 94305, USA; richard@slac.stanford.edu, ttanaka@slac.stanford.edu
[4] Santa Cruz Institute for Particle Physics, Department of Physics and Department of Astronomy and Astrophysics, University of California at Santa Cruz, Santa Cruz, CA 95064, USA
[5] Department of Astronomy, Stockholm University, SE-106 91 Stockholm, Sweden
[6] The Oskar Klein Centre for Cosmoparticle Physics, AlbaNova, SE-106 91 Stockholm, Sweden
[7] Istituto Nazionale di Fisica Nucleare, Sezione di Pisa, I-56127 Pisa, Italy
[8] Laboratoire AIM, CEA-IRFU/CNRS/Université Paris Diderot, Service d'Astrophysique, CEA Saclay, 91191 Gif sur Yvette, France
[9] Istituto Nazionale di Fisica Nucleare, Sezione di Trieste, I-34127 Trieste, Italy
[10] Dipartimento di Fisica, Università di Trieste, I-34127 Trieste, Italy
[11] Istituto Nazionale di Fisica Nucleare, Sezione di Padova, I-35131 Padova, Italy
[12] Dipartimento di Fisica "G. Galilei," Università di Padova, I-35131 Padova, Italy
[13] Department of Physics, Center for Cosmology and Astro-Particle Physics, The Ohio State University, Columbus, OH 43210, USA
[14] Istituto Nazionale di Fisica Nucleare, Sezione di Perugia, I-06123 Perugia, Italy
[15] Dipartimento di Fisica, Università degli Studi di Perugia, I-06123 Perugia, Italy
[16] Dipartimento di Fisica "M. Merlin" dell'Università e del Politecnico di Bari, I-70126 Bari, Italy
[17] Istituto Nazionale di Fisica Nucleare, Sezione di Bari, 70126 Bari, Italy
[18] Laboratoire Leprince-Ringuet, École polytechnique, CNRS/IN2P3, Palaiseau, France
[19] Department of Physics, University of Washington, Seattle, WA 98195-1560, USA
[20] INAF-Istituto di Astrofisica Spaziale e Fisica Cosmica, I-20133 Milano, Italy
[21] Agenzia Spaziale Italiana (ASI) Science Data Center, I-00044 Frascati (Roma), Italy
[22] NASA Goddard Space Flight Center, Greenbelt, MD 20771, USA; Robin.Corbet@nasa. gov
[23] Center for Research and Exploration in Space Science and Technology (CRESST), NASA Goddard Space Flight Center, Greenbelt, MD 20771, USA
[24] University of Maryland, Baltimore County, Baltimore, MD 21250, USA
[25] George Mason University, Fairfax, VA 22030, USA
[26] Laboratoire de Physique Théorique et Astroparticules, Université Montpellier 2, CNRS/IN2P3, Montpellier, France
[27] Department of Physics and Astronomy, Sonoma State University, Rohnert Park, CA 94928-3609, USA
[28] Department of Physics, Stockholm University, AlbaNova, SE-106 91 Stockholm, Sweden
[29] Dipartimento di Fisica, Università di Udine and Istituto Nazionale di Fisica Nucleare, Sezione di Trieste, Gruppo Collegato di Udine, I-33100 Udine, Italy
[30] Université Joseph Fourier-Grenoble 1/CNRS, laboratoire d'Astrophysique de Grenoble (LAOG) UMR 5571, BP 53, 38041 Grenoble Cedex 09, France; adam.hill@obs.ujf-grenoble.fr
[31] Université de Bordeaux, Centre d'Études Nucléaires Bordeaux Gradignan, UMR 5797, Gradignan, 33175, France
[32] CNRS/IN2P3, Centre d'Études Nucléaires Bordeaux Gradignan, UMR 5797, Gradignan, 33175, France
[33] Department of Physical Sciences, Hiroshima University, Higashi-Hiroshima, Hiroshima 739-8526, Japan
[34] University of Maryland, College Park, MD 20742, USA
[35] University of Alabama in Huntsville, Huntsville, AL 35899, USA
[36] Department of Physics, Tokyo Institute of Technology, Meguro City, Tokyo 152-8551, Japan

[37] Waseda University, 1-104 Totsukamachi, Shinjuku-ku, Tokyo, 169-8050, Japan
[38] Cosmic Radiation Laboratory, Institute of Physical and Chemical Research (RIKEN), Wako, Saitama 351-0198, Japan
[39] Centre d'Étude Spatiale des Rayonnements, CNRS/UPS, BP 44346, F-30128 Toulouse Cedex 4, France
[40] Istituto Nazionale di Fisica Nucleare, Sezione di Roma "Tor Vergata," I-00133 Roma, Italy
[41] Department of Physics and Astronomy, University of Denver, Denver, CO 80208, USA
[42] Max-Planck Institut für extraterrestrische Physik, 85748 Garching, Germany
[43] Institute of Space and Astronautical Science, JAXA, 3-1-1 Yoshinodai, Sagamihara, Kanagawa 229-8510, Japan
[44] Institut de Ciencies de l'Espai (IEEC-CSIC), Campus UAB, 08193 Barcelona, Spain
[45] Sterrenkundig Institut "Anton Pannekoek," 1098 SJ Amsterdam, Netherlands
[46] Institut für Astro- und Teilchenphysik and Institut für Theoretische Physik, Leopold-Franzens-Universität Innsbruck, A-6020 Innsbruck, Austria
[47] Department of Physics, Royal Institute of Technology (KTH), AlbaNova, SE-106 91 Stockholm, Sweden
[48] Space Sciences Division, NASA Ames Research Center, Moffett Field, CA 94035-1000, USA
[49] NYCB Real-Time Computing Inc., Lattingtown, NY 11560-1025, USA
[50] Department of Chemistry and Physics, Purdue University Calumet, Hammond, IN 46323-2094, USA
[51] Institució Catalana de Recerca i Estudis Avançats, Barcelona, Spain
[52] Consorzio Interuniversitario per la Fisica Spaziale (CIFS), I-10133 Torino, Italy
[53] North-West University, Potchefstroom Campus, Potchefstroom 2520, South Africa
[54] Dipartimento di Fisica, Università di Roma "Tor Vergata," I-00133 Roma, Italy
[55] School of Pure and Applied Natural Sciences, University of Kalmar, SE-391 82 Kalmar, Sweden
Received 2009 September 18; accepted 2009 October 9; published 2009 October 30

ABSTRACT

The first results from observations of the high-mass X-ray binary LS 5039 using the *Fermi Gamma-ray Space Telescope* data between 2008 August and 2009 June are presented. Our results indicate variability that is consistent with the binary period, with the emission being modulated with a period of 3.903 ± 0.005 days; the first detection of this modulation at GeV energies. The light curve is characterized by a broad peak around superior conjunction in agreement with inverse Compton scattering models. The spectrum is represented by a power law with an exponential cutoff, yielding an overall flux (100 MeV–300 GeV) of $4.9 \pm 0.5\text{(stat)} \pm 1.8\text{(syst)} \times 10^{-7}$ photon cm^{-2} s^{-1}, with a cutoff at $2.1 \pm 0.3\text{(stat)} \pm 1.1\text{(syst)}$ GeV and photon index $\Gamma = 1.9 \pm 0.1\text{(stat)} \pm 0.3\text{(syst)}$. The spectrum is observed to vary with orbital phase, specifically between inferior and superior conjunction. We suggest that the presence of a cutoff in the spectrum may be indicative of magnetospheric emission similar to the emission seen in many pulsars by *Fermi*.

Key words: binaries: close – gamma rays: observations – stars: variables: other – X-rays: binaries – X-rays: individual (LS 5039)

1. INTRODUCTION

LS 5039, PSR B1259−63 and LS I +61°303 are the only binaries with high-mass companions long known to be spatially coincident with sources detected at energies greater than 100 MeV, e.g., those listed in the Third Energetic Gamma-Ray Experiment (EGRET) catalog (Hartman et al. 1999). The latter binary was detected by the Large Area Telescope (LAT) on the *Fermi* mission, confirming it as a GeV gamma-ray source and finding variability that is consistent with modulation on the binary period of 26.6 ± 0.5 days (Abdo et al. 2009b). This constituted the first detection of orbital periodicity in high-energy (HE) gamma rays (20 MeV–100 GeV). In this Letter, we present the results of *Fermi* observations of LS 5039.

LS 5039 is one of a handful of X-ray binaries that have been detected recently at very high-energy γ-rays; results from ∼70 hr of observations distributed over many orbital cycles have been presented by Aharonian et al. (2005b, 2006). These observations yielded a modulation of the very high energy (VHE, >100 GeV) gamma-ray flux with a period of 3.9078 ± 0.0015 days (Aharonian et al. 2006), consistent with the orbital period as determined by Casares et al. (2005) from optical spectroscopy. Short timescale variability displayed on top of this periodic behavior, both in the flux and the spectrum, was also reported.

The nature of the LS 5039 compact object is unknown: a black hole and a neutron star have been invoked as possible compact object companions in a slightly eccentric ($e \sim 0.35$), 3.90603 ± 0.00017 day orbit around the O6.5V star (Casares et al. 2005). The discovery of a jet-like radio structure in LS 5039 coincident with an X-ray and EGRET source prompted a microquasar interpretation (Paredes et al. 2000a). Variability in the EGRET source could not be established precisely (Torres et al. 2001; Nolan et al. 2003). Recently, it has been shown that the X-ray flux is modulated on the orbital period (Takahashi et al. 2009).

Ribó et al. (2008) provided Very Long Baseline Array (VLBA) radio observations of LS 5039 with morphological and astrometric information at milliarcsecond scales that cannot easily be explained by a microquasar scenario. Martocchia et al. (2005) assessed the low X-ray state, showing the absence of accretion features in the X-ray spectra. Thus, measurements at radio and VHE γ-rays in the cases of LS I +61°303 (Dhawan et al. 2006; Albert et al. 2008) or PSR B1259−63 (Aharonian et al. 2005a), whose overall spectral energy distribution is similar to that of LS 5039, gave the impression that all three systems are different realizations of the same scenario: a pulsar-massive star binary (Dubus 2006b).

Theoretical computations of the gamma-ray emission in both compact object scenarios have been made, with gamma rays produced by inverse Compton (IC) scattering of the stellar light by VHE electrons accelerated in the vicinity of the compact object. In the case of the black hole companion, HE and VHE emission would result from particles accelerated in the jet (Bednarek 2007a; Böttcher 2007; Khangulyan et al. 2008). Alternatively, it would involve the relativistic wind of a young, rotation-powered pulsar, either as a result of particle acceleration in the wind interaction region (Dubus 2006b) or by processes

[56] Royal Swedish Academy of Sciences Research Fellow, funded by a grant from the K. A. Wallenberg Foundation.
[57] Funded by contract ERC-StG-200911 from the European Community.

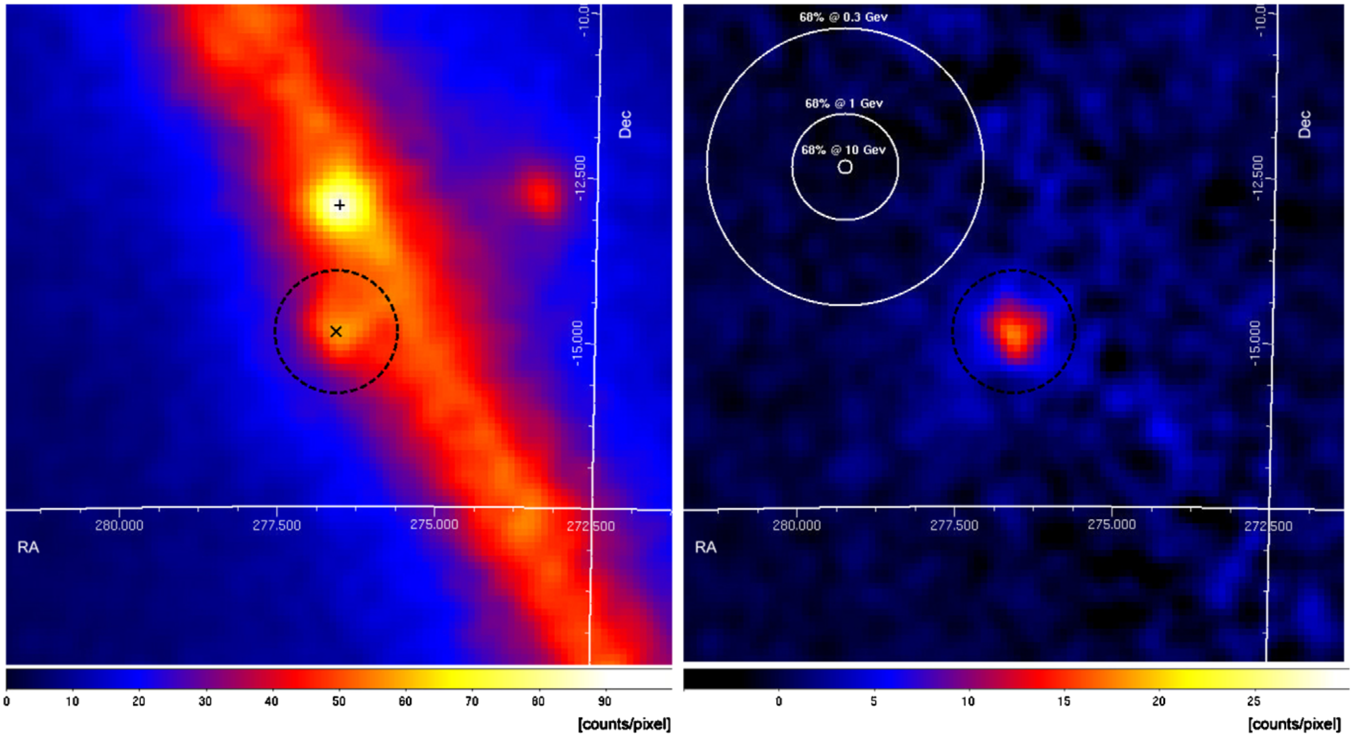

Figure 1. Left: the smoothed counts map for 100 MeV–300 GeV of a $10^\circ \times 10^\circ$ region around the LS 5039 location (marked with "×"); the dashed black circle indicates the $0\overset{\circ}{.}925$ timing analysis aperture. A $0\overset{\circ}{.}3$ Gaussian smoothing function was applied to the $0\overset{\circ}{.}1$ bins. PSR J1826−1256 is marked with "+." The exposure varies by less than 7% across the field at a representative energy of 10 GeV. Right: residuals of left panel after subtracting all modelled sources excluding LS 5039 and excluding events which arrive during the peaks in the pulsar phase cycle of PSR J1826−1256 (see Section 4). The white circles indicate the 68% LAT containment region at three energies: 0.3, 1, and 10 GeV. Note that the color scales are different for the two panels.

within the pulsar wind (Sierpowska-Bartosik & Torres 2008a, 2008b; Cerutti et al. 2008).

2. DATA REDUCTION AND RESULTS

The LAT onboard *Fermi* is an electron–positron pair production telescope, featuring solid state silicon trackers and cesium iodide calorimeters, sensitive to photons from ∼20 MeV to > 300 GeV (Atwood et al. 2009).

The analysis data set spanned 2008 August 4 through 2009 June 22. The data were reduced and analyzed using the Fermi Science Tools v9r15 package.[58] The standard onboard filtering, event reconstruction, and classification were applied to the data (Atwood et al. 2009), and for this analysis the high-quality ("Pass 6 diffuse") event class is used. Throughout the analysis, the "Pass 6 v3 Diffuse" (P6_V3_DIFFUSE) instrument response functions (IRFs) are applied.

Time periods when the region around LS 5039 was observed at a zenith angle greater than 105° and for observatory rocking angles of greater than 43° were also excluded to avoid contamination from the Earth albedo photons. With these cuts, a photon count map of a 10° region around the binary is shown in Figure 1.

LS 5039 is detected at a level of 28.5σ (see Section 4). The `gtfindsrc` tool finds a best-fit location for LS 5039 of R.A. $= 18^{\rm h}26^{\rm m}24\overset{\rm s}{.}7$, decl. $= -14^\circ 48' 39''$(J2000) with a 95% error of 0.054° (including a 20% systematic error derived from the internal *Fermi* 11-month catalog). The nominal position of LS 5039 at R.A. $= 18^{\rm h}26^{\rm m}15\overset{\rm s}{.}1$, decl. $= -14^\circ 50' 54\overset{''}{.}3$ (J2000) (Zacharias et al. 2004) lies just on the *Fermi* 95% contour; the nominal position was used throughout the analysis.

3. TIMING ANALYSIS

LAT light curves were extracted using aperture photometry. The LAT point-spread function (PSF) is strongly energy dependent and, particularly since LS 5039 is located in the Galactic plane, there is also significant contribution to flux within an aperture from diffuse emission and point sources that depends on the aperture size and the energy range used. The aperture and energy band employed were independently chosen to maximize the signal-to-noise level. The optimum aperture radius was found to be approximately $0\overset{\circ}{.}925$ in the energy range 100 MeV–10 GeV. The time binning of the light curve was 1000 s. Exposures were calculated using `gtexposure` assuming a power-law spectrum with a photon index of $\Gamma = 2.5$.

A search was made for periodic modulation by calculating the weighted periodogram of the light curve (Lomb 1976; Scargle 1982; Corbet & Dubois 2007). Since the exposure of the time bins was variable, the contribution of each time bin to the power spectrum was weighted based on its relative exposure. The periodogram is shown in Figure 2. The arrow marks the Casares et al. (2005) orbital period and a highly significant peak is detected at this period; the false alarm probability is $\sim 10^{-10}$. The significance levels marked are for a "blind" search with 5000 independent frequency steps, however, the effects of the tuning of the aperture radius and energy range are not taken into account. The period error was estimated using a Monte Carlo approach: light curves were simulated using the observed LS 5039 light curve and randomly shuffling the data points within their errors, assuming Gaussian statistics. The

[58] See the FSSC website for details of the Science Tools: http://fermi.gsfc.nasa.gov/ssc/data/analysis/.

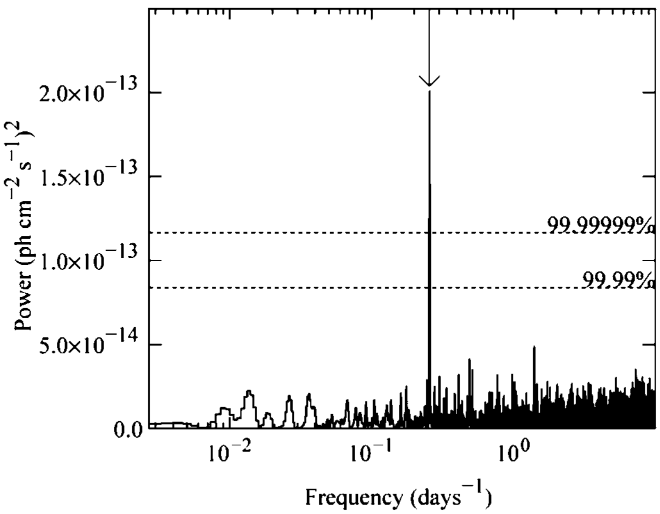

Figure 2. Power spectrum of the light curve. The arrow indicates the known orbital period of 3.90603 days (Casares et al. 2005). The dashed lines show the 99.99% and 99.99999% significance levels.

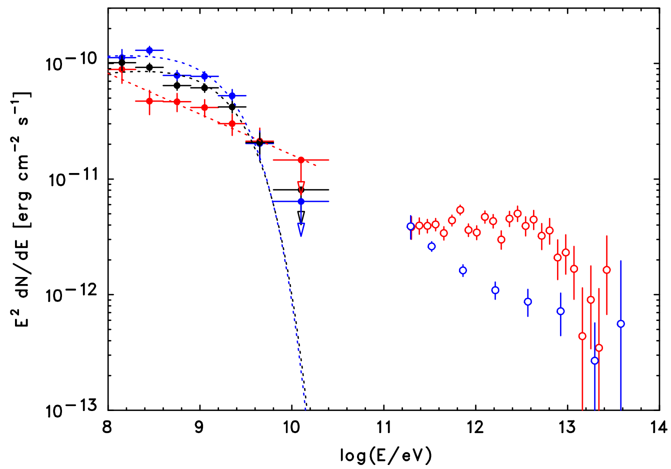

Figure 3. Fitted spectrum of LS 5039. Fermi data points are from likelihood fits in each energy bin. The black points (dotted line) represent the phase-averaged *Fermi*/LAT spectrum. The red data points (dotted line) represent the spectrum (overall fit) at inferior conjunction (Phase 0.45–0.9); blue data points (dotted line) represent the spectrum (overall fit) at superior conjunction (Phases < 0.45 and > 0.9). Data points above 100 GeV are taken from H.E.S.S. observations (Aharonian et al. 2006); the data from H.E.S.S. are not contemporaneous with *Fermi*, though they do cover multiple orbital periods.

corresponding periodogram was then calculated and the location of the peak at ∼3.9 days recorded. From ∼200,000 simulations, we calculate an error estimate of the orbital period of 3.903 ± 0.005 days (1σ).

4. SPECTRAL ANALYSIS

The `gtlike` likelihood fitting tool was used to perform the spectral analysis, wherein a spectral-spatial model containing point and diffuse sources is created and the parameters obtained from a simultaneous maximum likelihood fit to the data. The 10° region around the source was modeled for Galactic and isotropic diffuse contributions and 22 additional significant point sources (taken from the internal *Fermi* 11-month catalog) were included; point sources were modeled with simple power laws with the exception of the bright, nearby pulsar (PSR J1826−1256) for which a power law with an exponential cutoff was used. The flux contribution of PSR J1826−1256 to the region was minimized by excluding events which arrive during the peaks in the pulsar phase cycle ($0.175 < \phi < 0.3$ and $0.625 < \phi < 0.775$ were excluded; see Abdo et al. 2009a). A scaling factor of $1/0.725$ is applied to measured fluxes to account for livetime loss due to this cut.

The 10° region was chosen to capture the broad PSF obtained at 100 MeV. An alternate fitting method using energy-dependent regions of interest was used, yielding compatible results that were folded into the systematic errors.

In analyzing the emission of LS 5039, we used models for the Galactic diffuse emission ($gll\_iem\_v02.fit$) and isotropic backgrounds currently recommended by the LAT team.[59] The model for the Galactic diffuse emission was developed using spectral line surveys of H I, CO (as a tracer of H_2) to derive the distribution of interstellar gas in Galactocentric rings.

The model of the diffuse gamma-ray emission was then constructed by fitting the gamma-ray emissivities of the rings in several energy bands to the LAT observations. The fitting also required a model of the IC emission calculated using GALPROP (Strong 2007) and a model for the isotropic diffuse emission. The latter was fitted to the LAT data using an analysis of the sky above $|b| = 30°$ and includes the significant contribution of residual (misclassified) cosmic rays at high energies for the current IRFs.

Initially a simple power law, $E^{-\Gamma}$, was fitted to the data from all orbital phases yielding a photon index of $\Gamma \sim 2.54$. However, as can be clearly seen in Figure 3, the energy spectrum appears to turn over at energies above ∼2 GeV. The possibility of an exponential cutoff was investigated in the form $E^{-\Gamma} \exp[-(E/E_{\rm cutoff})]$. The chance probability to incorrectly reject the power-law hypothesis was found to be 1.6×10^{-16}. The maximum likelihood exponential cutoff spectral model has a likelihood test statistic (Mattox et al. 1996) value of ∼814.6, or 28.5σ. The photon index is $\Gamma = 1.9 \pm 0.1$ (stat) $\pm$ 0.3(syst); the 100 MeV– 300 GeV flux is $(4.9 \pm 0.5$ (stat) $\pm$ 1.8 (syst)) $\times 10^{-7}$ photon cm^{-2} s^{-1} and the cutoff energy is 2.1 ± 0.3 (stat)$\pm$ 1.1(syst)GeV (see below for a discussion of systematics). The correlation between the photon index and cutoff energy was explored by fitting a family of models over a grid of indices and cutoff energies centered on the best-fit parameter values. The 1σ, 2σ, and 3σ error contours are shown in Figure 4; both parameters are bounded and well constrained. A total of 359,789 photons were found in the 10° region. Evaluating the fit parameters, 3992 ± 63 photons were observed from LS 5039 above 100 MeV.

A number of effects are expected to contribute to the systematic errors. The largest is uncertainty in the diffuse modeling as evidenced by the intense swath of photons along the Galactic plane shown in Figure 1. A reasonable range of shape difference has been explored using the GALPROP model of the region. Both models give reasonable residuals maps and show differences of 10%, 37%, and 50%, respectively, for index, cutoff energy and flux. In all diffuse models tested, the exponential cutoff model is a significant improvement over the power law.

The impact of systematic uncertainties due to the IRFs are estimated by using outlier IRFs that bracket our nominal ones in effective area. These are defined by envelopes above and below the P6_V3 IRFs by linearly connecting differences of (10%, 5%, and 20%) at $\log(E/\text{MeV})$ of (2, 2.75, and 4), respectively. The variation on the index was 15%; the other parameter variations

[59] Descriptions of the models are available from the FSSC: http://fermi.gsfc.nasa.gov/.

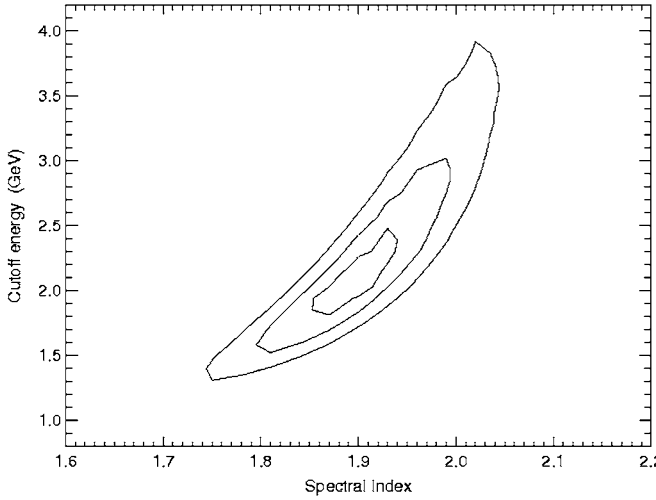

Figure 4. 1σ, 2σ, and 3σ contours for the photon index and cutoff energy spectral parameters from fitting to the phase-averaged *Fermi* data.

were small compared to those due to the diffuse modeling. Other effects considered are fitting technique, cuts applied (minimum and maximum energies), but they are all within the ranges defined by diffuse modeling and bracketing effective area variations.

4.1. Phase-Resolved Spectral Analysis

We also searched for orbital dependence of the spectral shape. `gtlike` fits were performed for each phase interval of $\Delta\phi = 0.1$ in the same way as for the phase-averaged spectral analysis. Figure 5 shows the hardness ratio, $F_{1-100\,\text{GeV}}/F_{0.1-1\,\text{GeV}}$, as a function of orbital phase. Due to limited statistics, bin widths of $\Delta\phi$ of 0.2 are used for the phase interval $\phi = 0.3$–0.6, while $\Delta\phi = 0.1$ are employed for the other phase intervals. The spectral shape varied such that the spectrum is softer around periastron and is harder around apastron.

Aharonian et al. (2006) define two broad phase intervals, inferior conjunction ($0.45 < \phi < 0.9$) and superior conjunction ($0.9 < \phi < 0.45$), both H.E.S.S. spectra being shown in Figure 3. Taking the same phase intervals with the LAT data, we find a power-law spectrum with $\Gamma = 2.25 \pm 0.11$ at inferior conjunction; an energy cutoff was not statistically justified. At superior conjunction, a power law with an exponential cutoff was preferred with $\Gamma = 1.91 \pm 0.16$ and a cutoff energy of 1.9 ± 0.5 GeV. Aharonian et al. (2006) report spectral variability in the source between superior and inferior conjunction, however, they do not see any indication of long-term variability suggesting that it may be reasonable to compare non-contemporaneous observations.

5. DISCUSSION

The initial association of LS 5039 with the EGRET source 3EG J1824−1514 (Paredes et al. 2000b) had remained tentative due to the large EGRET error circle and the lack of timing signatures. The association was bolstered by the discovery of point-like, modulated gamma-ray emission above 100 GeV (Aharonian et al. 2005b, 2006). The *Fermi* observations enabled the detection of an orbital modulation, indicating that the binary is also a source of gamma rays above 100 MeV. The periods determined independently from the *Fermi*-LAT and H.E.S.S. data are self consistent and compatible with the binary period obtained from radial velocity measurements of the companion

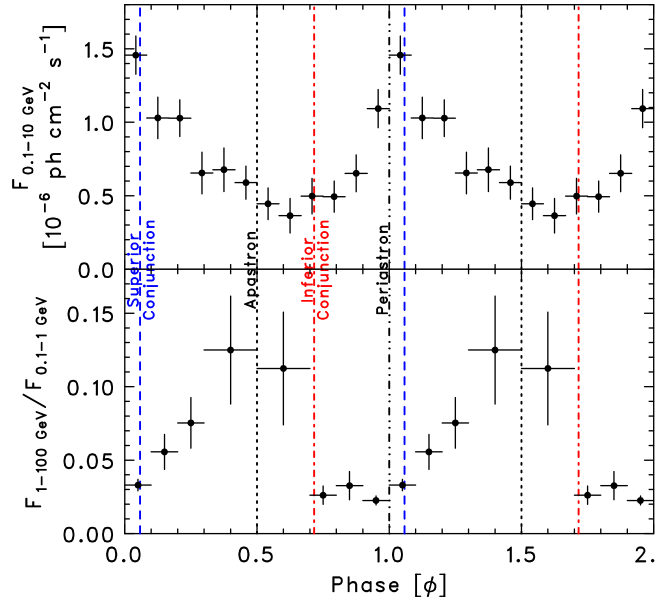

Figure 5. Top: flux vs. orbital phase for 0.1–10 GeV. Bottom: variations with orbital phase in the hardness ratio of 1–100 to 0.1–1 GeV.

(Aragona et al. 2009). This is only the second high-mass X-ray binary after LS I +61°303 (Abdo et al. 2009b) to become a confirmed emitter in the HE gamma-ray domain.

The short orbital period means that the compact object passes within a stellar radius of the surface of the $kT_\star \approx 3$ eV, $R_\star \approx 10\,R_\odot$ companion (Casares et al. 2005). Gamma rays emitted in the vicinity of the compact object with energies above the 30 GeV threshold inevitably pair produce with stellar photons (see, e.g., Protheroe & Stanev 1987; Moskalenko 1995; Böttcher & Dermer 2005; Dubus 2006a). Emission in the *Fermi* range is largely unaffected by absorption and should allow easier identification of the intrinsic spectrum and variability of the source. However, it can be affected by cascading of higher-energy photons.

The HE modulation peaks at $\phi \sim 0.0$–0.1, close to superior conjunction ($\phi = 0.06$) while the VHE modulation peaks close to inferior conjunction ($\phi = 0.72$). The phase difference can be explained mostly as a result of the competition between IC scattering on high-energy electrons and VHE pair production, assuming the companion star to be close to the compact object. The star provides target photons for both processes with the radiation density varying by a factor 4 along the eccentric orbit. IC scattering will vary with radiation density but, because the source of seed photons is anisotropic, the flux will also depend on the geometry seen by the observer in non-trivial ways (Khangulyan et al. 2008; Sierpowska-Bartosik & Torres 2008b). The emission is enhanced (reduced) when the highly relativistic electrons seen by the observer encounter the seed photons head-on (rear-on), i.e., at superior (inferior) conjunction. Inversely, VHE absorption due to pair production will be maximum (minimum) at superior (inferior) conjunction. The phases of minimum and maximum flux in *Fermi* as well as the anti-correlation with H.E.S.S. are consistent with these expectations, suggesting IC scattering is the dominant radiative process above 100 MeV with the additional effect of pair production above 30 GeV (Bednarek 2007b; Dubus et al. 2008; Sierpowska-Bartosik & Torres 2008a). It is, however, yet unclear whether the IC VHE emission is mainly produced already in the pulsar wind zone of the system, given the high opacity already found therein for particles accelerated at the pulsar site (Sierpowska-

Bartosik & Torres 2008b) or as a result of particle acceleration at the shock formed in the wind collision region (Dubus 2006a) or even well beyond the system (Bosch-Ramon et al. 2008).

However, the extension of these pictures from the TeV into the GeV domain is undermined by the presence of an exponential cutoff at a few GeV in the *Fermi* spectrum. A cutoff at ∼6.3 GeV was also observed in LS I +61°303 indicating that this may be a common spectral feature in this class of source. The companion star in LS I +61°303 is a Be star with a dense equatorial disk. Passage of the compact object through this disk might have explained the exponential cutoff: for instance, this would crush a putative pulsar wind nebula closer to the neutron star, increasing synchrotron losses and introducing a strong dependence with orbital phase of the electron energy distribution (Dubus 2006b). But there is no such large, systematic contrast in the density of the stellar wind from the O6.5V star along the orbit in LS 5039. The presence of a similar cutoff in both systems argues against explanations related to the properties of the orbit or companion star. The cutoff seems to require that the radiative process or radiating electrons be different between the HE and VHE domains, in disagreement with the picture presented above.

An intriguing possibility is that the emission in the *Fermi* range from both LS 5039 and LS I +61°303 is magnetospheric emission as seen in the dozens of pulsars that have now been detected by *Fermi*. The typical *Fermi* pulsar emission has a hard power-law spectrum with a photon index ≈1.5 and an exponential cutoff at ≈2.5 GeV. In this case, the cutoff energy is thought to be set by the balance between acceleration and losses to curvature radiation. The emission should in such a case be pulsed, although the orbital motion makes it exceedingly difficult to find in the *Fermi* data with no prior knowledge of the spin period. Pulsar wind emission would dominate in the neighboring hard X-ray and VHE bands, supported by their similar orbital modulations (Hoffmann et al. 2009; Takahashi et al. 2009). It is to be noted that there is, however, an issue associated with having dominant magnetospheric emission in the HE band: magnetospheric emission is usually thought to be due to curvature radiation and has no obvious reason to be modulated with the orbital motion (although magnetospheric emission from pulsars in close binaries has hardly been modeled). The dense photon environment of the binaries may perhaps introduce differences compared to gamma-ray magnetospheric emission from isolated pulsars (for instance, in the pair multiplicity). Hence, the spectrum suggests a magnetospheric emission interpretation, which is hard to reconcile with the IC scattering interpretation suggested by the modulation. Future HE and VHE should lead to better constraints on the variability of the spectral parameters along the orbit. This will help resolve whether there are several components and what their relative amplitudes are.

The *Fermi*/LAT Collaboration acknowledges generous ongoing support from a number of agencies and institutes that have supported both the development and the operation of the LAT as well as scientific data analysis. These include the National Aeronautics and Space Administration and the Department of Energy in the United States; the Commissariat à l'Energie Atomique and the Centre National de la Recherche Scientifique/Institut National de Physique Nucléaire et de Physique des Particules in France; the Agenzia Spaziale Italiana and the Istituto Nazionale di Fisica Nucleare in Italy; the Ministry of Education, Culture, Sports, Science and Technology (MEXT), High Energy Accelerator Research Organization (KEK), and Japan Aerospace Exploration Agency (JAXA) in Japan; and the K. A. Wallenberg Foundation, the Swedish Research Council, and the Swedish National Space Board in Sweden.

Additional support for science analysis during the operations phase is gratefully acknowledged from the Spanish CSIC and MICINN, the Istituto Nazionale di Astrofisica in Italy and the Centre National d'Études Spatiales in France.

Facility: Fermi

REFERENCES

Abdo, A. A., et al. 2009a, Science, 325, 840
Abdo, A. A., et al. 2009b, ApJ, 701, L123
Aharonian, F., et al. 2005a, A&A, 442, 1
Aharonian, F., et al. 2005b, Science, 309, 746
Aharonian, F., et al. 2006, A&A, 460, 743
Albert, J., et al. 2008, ApJ, 684, 1351
Aragona, C., McSwain, M. V., Grundstrom, E. D., Marsh, A. N., Roettenbacher, R. M., Hessler, K. M., Boyajian, T. S., & Ray, P. S. 2009, ApJ, 698, 514
Atwood, W. B., et al. 2009, ApJ, 697, 1071
Bednarek, W. 2007a, A&A, 464, 259
Bednarek, W. 2007b, A&A, 464, 259
Bosch-Ramon, V., Khangulyan, D., & Aharonian, F. A. 2008, A&A, 489, L21
Böttcher, M. 2007, Astropart. Phys., 27, 278
Böttcher, M., & Dermer, C. D. 2005, ApJ, 634, L81
Casares, J., Ribó, M., Ribas, I., Paredes, J. M., Martí, J., & Herrero, A. 2005, MNRAS, 364, 899
Cerutti, B., Dubus, G., & Henri, G. 2008, A&A, 488, 37
Corbet, R., & Dubois, R. 2007, in AIP Conf. Ser. 921, The First GLAST Symp., ed. S. Ritz, P. Michelson, & C. A. Meegan (Melville, NY: AIP), 548
Dhawan, V., Mioduszewski, A., & Rupen, M. 2006, in Proc. VI Microquasar Workshop: Microquasars and Beyond, ed. T. Belloni, PoS(MQW6)052
Dubus, G. 2006a, A&A, 451, 9
Dubus, G. 2006b, A&A, 456, 801
Dubus, G., Cerutti, B., & Henri, G. 2008, A&A, 477, 691
Hartman, R. C., et al. 1999, ApJS, 123, 79
Hoffmann, A. D., Klochkov, D., Santangelo, A., Horns, D., Segreto, A., Staubert, R., & Puehlhofer, G. 2009, A&A, 494, L37
Khangulyan, D., Aharonian, F., & Bosch-Ramon, V. 2008, MNRAS, 383, 467
Lomb, N. R. 1976, Ap&SS, 39, 447
Martocchia, A., Motch, C., & Negueruela, I. 2005, A&A, 430, 245
Mattox, J. R., et al. 1996, ApJ, 461, 396
Moskalenko, I. V. 1995, Space Sci. Rev., 72, 593
Nolan, P. L., Tompkins, W. F., Grenier, I. A., & Michelson, P. F. 2003, ApJ, 597, 615
Paredes, J. M., Martí, J., Ribó, M., & Massi, M. 2000a, Science, 288, 2340
Paredes, J. M., Martí, J., Ribó, M., & Massi, M. 2000b, Science, 288, 2340
Protheroe, R. J., & Stanev, T. 1987, ApJ, 322, 838
Ribó, M., Paredes, J. M., Moldón, J., Martí, J., & Massi, M. 2008, A&A, 481, 17
Scargle, J. D. 1982, ApJ, 263, 835
Sierpowska-Bartosik, A., & Torres, D. F. 2008a, ApJ, 674, L89
Sierpowska-Bartosik, A., & Torres, D. F. 2008b, Astropart. Phys., 30, 239
Strong, A. W. 2007, Ap&SS, 309, 35
Takahashi, T., et al. 2009, ApJ, 697, 592
Torres, D. F., Romero, G. E., Combi, J. A., Benaglia, P., Andernach, H., & Punsly, B. 2001, A&A, 370, 468
Zacharias, N., Urban, S. E., Zacharias, M. I., Wycoff, G. L., Hall, D. M., Monet, D. G., & Rafferty, T. J. 2004, AJ, 127, 3043